

Introduction

Prediction and control of the onset of transition and the associated variation in aerothermodynamic parameters in high-speed flows is key to optimize the performance and design of Thermal Protection Systems (TPS) of next-generation aerospace vehicles [1]. Boundary Layer Transition (BLT) characteristics can influence the surface heating budget determining the TPS thickness and consequently its weight penalty. Ablative heatshields are designed to alleviate the high heat flux at the surface through pyrolysis of their polymeric matrix and subsequent fiber ablation [2]. Pyrolysis leads to out-gassing and non-uniform ablation lead to surface roughness, both of which are known to influence the transition process. An ablator impacts BLT through three main routes: gas injecting into the boundary layer from the wall, changing the surface heat transfer due to wall-flow chemical reactions, and modifying surface roughness [3]. In preparation to Mars 2020 mission post-flight analysis, the predictive transition capability has been initiated toward hard-coupling porous material response analysis and aerothermal environment calculation.

Methodology

To develop correlations for transition induced by the ablation product boundary layer interaction, we start with the simplest form of a smooth but blowing surface. The effect of out-gassing associated with surface pyrolysis on the onset of transition is examined by employing the concept of intermittency γ as a measure of the probability that the flow is turbulent at a given point in space and time [4]. A surface map of intermittency is created such that the change in pressure gradient from favorable to adverse near the stagnation-point region, marked in dashed region of Fig. 1 (a), corresponds to the high-intermittency region as shown in Fig. 1 (b).

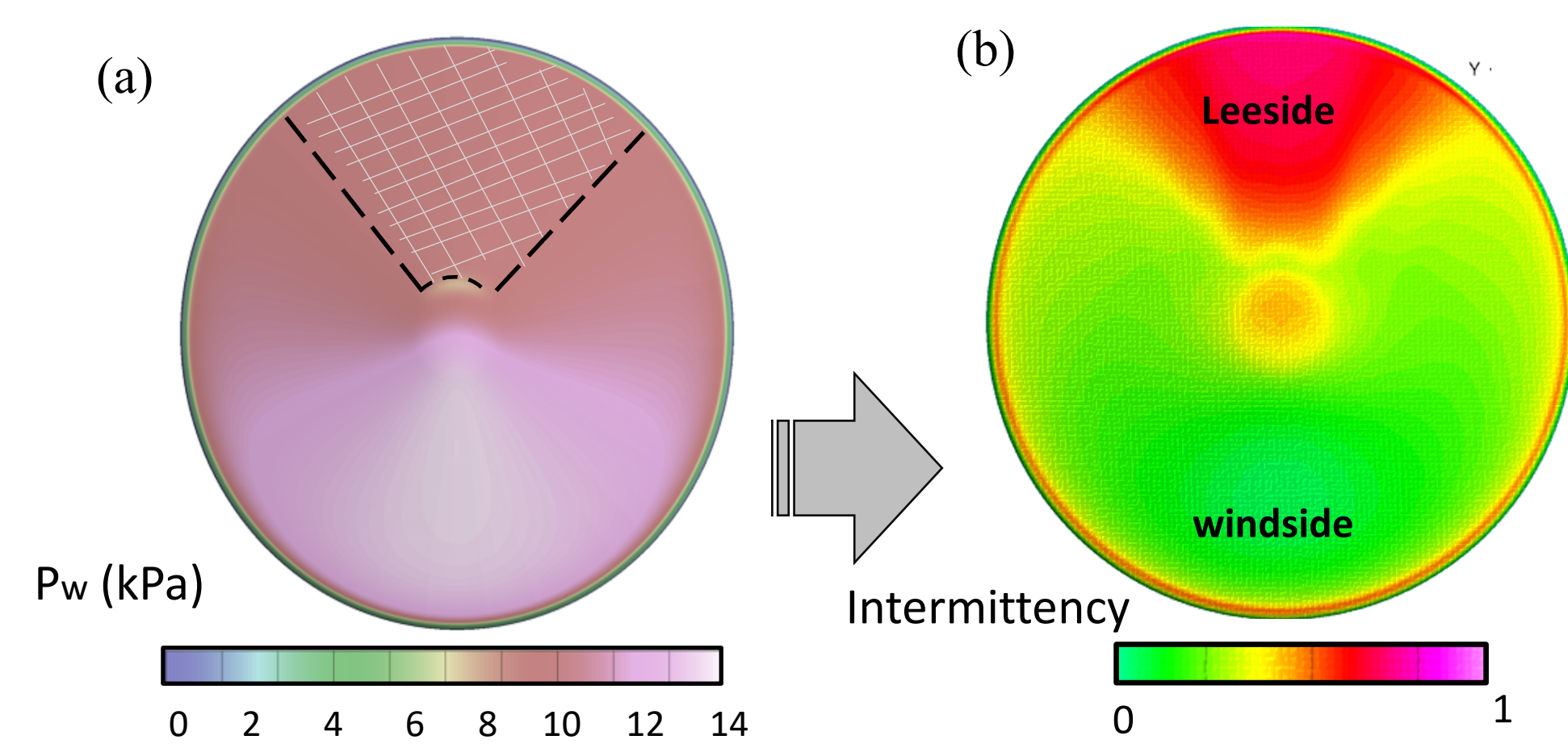


Fig. 1 Wall pressure (a) and intermittency distribution (b) on the forebody at 74 s along the flight trajectory

Although the blowing rate is not uniformly constant across the wetted face of the heatshield, as a first approximation, we assume that the gas constantly blown into the boundary layer is only present where maximum wall heat flux has been observed and is associated with higher γ in the transition map. To model the effect of ablation-induced out-gassing on transition onset, we compare non-injecting gas boundary layer as a baseline case with the cases with various

blowing rates. Injecting gas is applied to the regions of the wetted surface where transition has been observed in the previous flight data (**Scenario A**). Similarly, series of numerical experiments are conducted for laminar, transitional and turbulent regimes of flows assuming there is continuously

uniform blowing on the entire forebody surface area (**Scenario B**). We here examine injecting the same gas mixture as that of the freestream. Blowing rate is characterized by a non-dimensional parameter F_w

$$F_w = (\rho_e u_e A_{tot})^{-1} \int_0^{A_w} \rho_w v_w dA$$

such that the blowing surface areas (A_w) and only vertical component of velocity at the wall are considered. The surface is assumed to be in radiative equilibrium, fully

catalytic to ions, but supports only homogeneous surface reactions. Using the CFD code Data Parallel Line Relaxation (DPLR) [5] for the continuum phase of entry, an extensive series of simulations has been conducted to understand the role of blowing rate on different regimes of flow. We employ the finite chemistry model with 18 species [6] and model turbulence using the shear stress transport model with compressibility correction [7] while the production of turbulent kinetic energy is weighted by intermittency distribution.

Results

Turbulent augmentation of heat flux $\phi = q_{w,turb}/q_{w,lam}$ due to out-gassing is more enhanced when blowing corresponds to the transition map and γ distribution as shown in Fig. 2. The integral quantities such as the momentum thickness shown in Fig. 3 can give insight to cor-

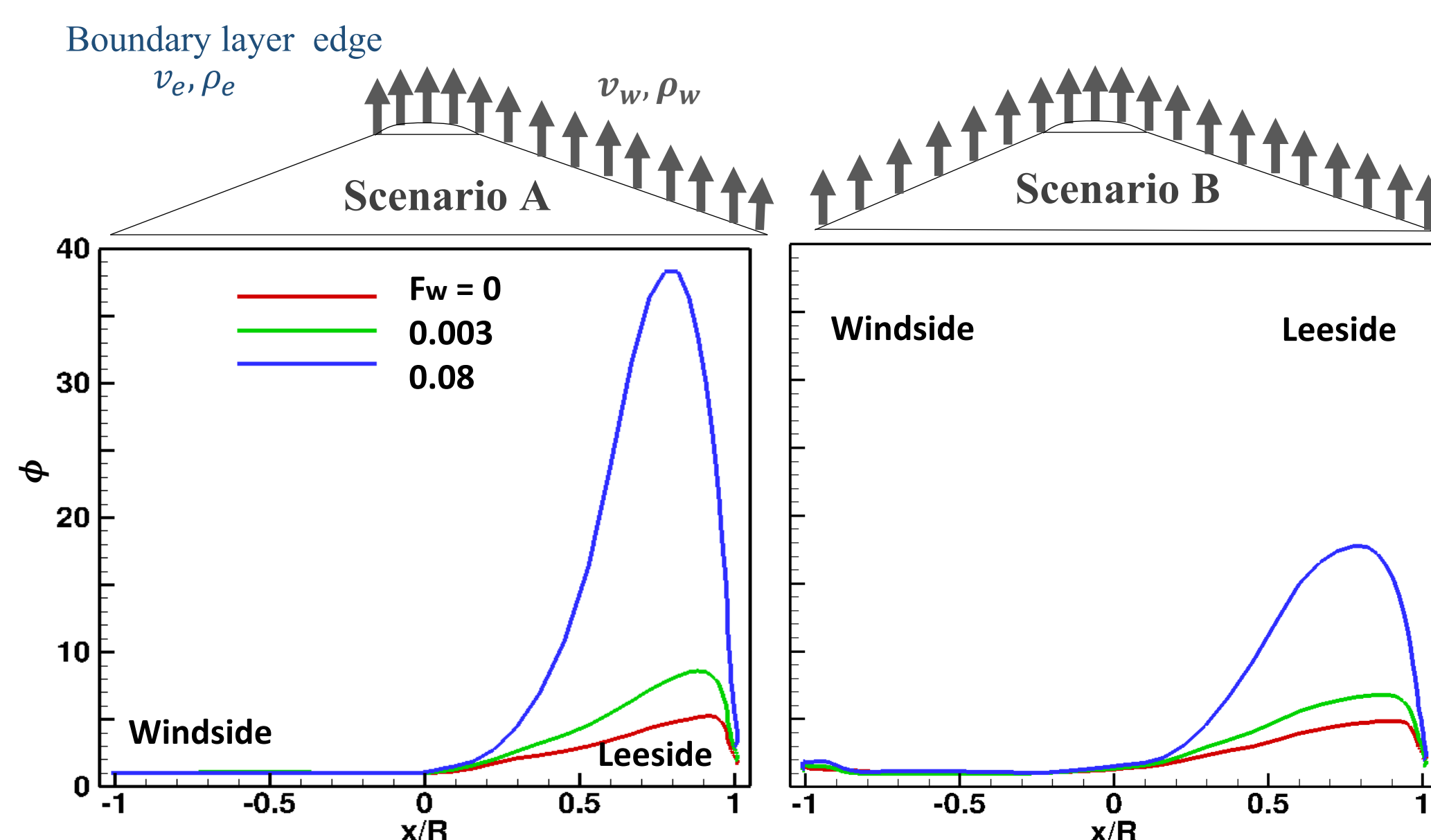


Fig. 2 Turbulent augmentation of convective heat flux due to the wall blowing for Scenario A (left) and Scenario B (right)

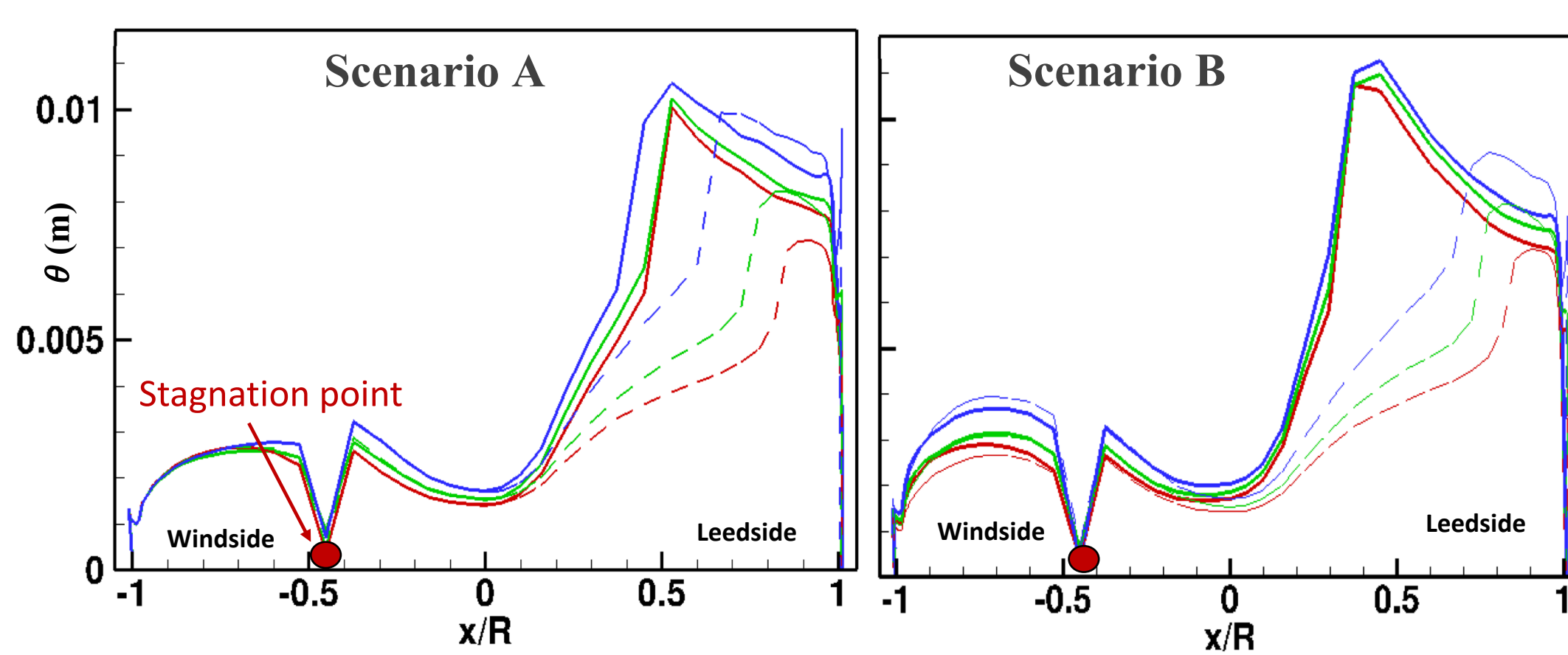


Fig. 3 Centerline profile of momentum thickness with different blowing parameters (Legend similar to Fig.4)

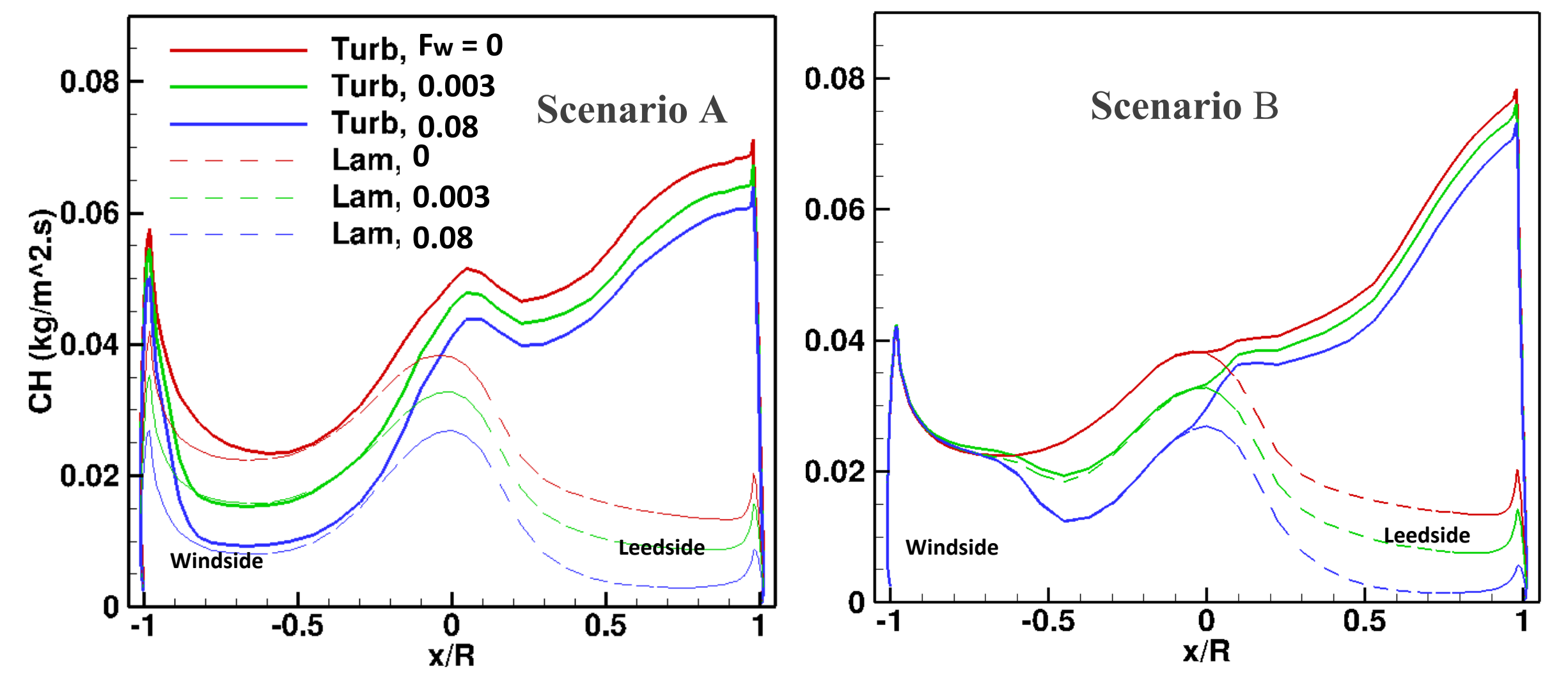


Fig. 4 Centerline profile of heat transfer coefficient for with different blowing parameters at 75 s along the flight trajectory

relate wall temperature and blowing rate determining the transition onset. Although here we only present the results at the time of peak heating (75 s), we need to consider the trajectory interval where turbulent bump factor is larger than unity [8] in order to capture the temporal evolution of transition location via such a correlation. Stronger out-gassing (Scenario A) inhibits the wall heat transfer coefficient and moves the transition location toward the windside as shown in Fig. 4. Regardless of the blowing rate, no significant difference between the Stanton number of the laminar and turbulent solutions on the windside of the forebody has been observed. Fig. 5 shows that laminar flows compared to turbulent and transitional counterparts experiences more wall cooling due to out-gassing effects.

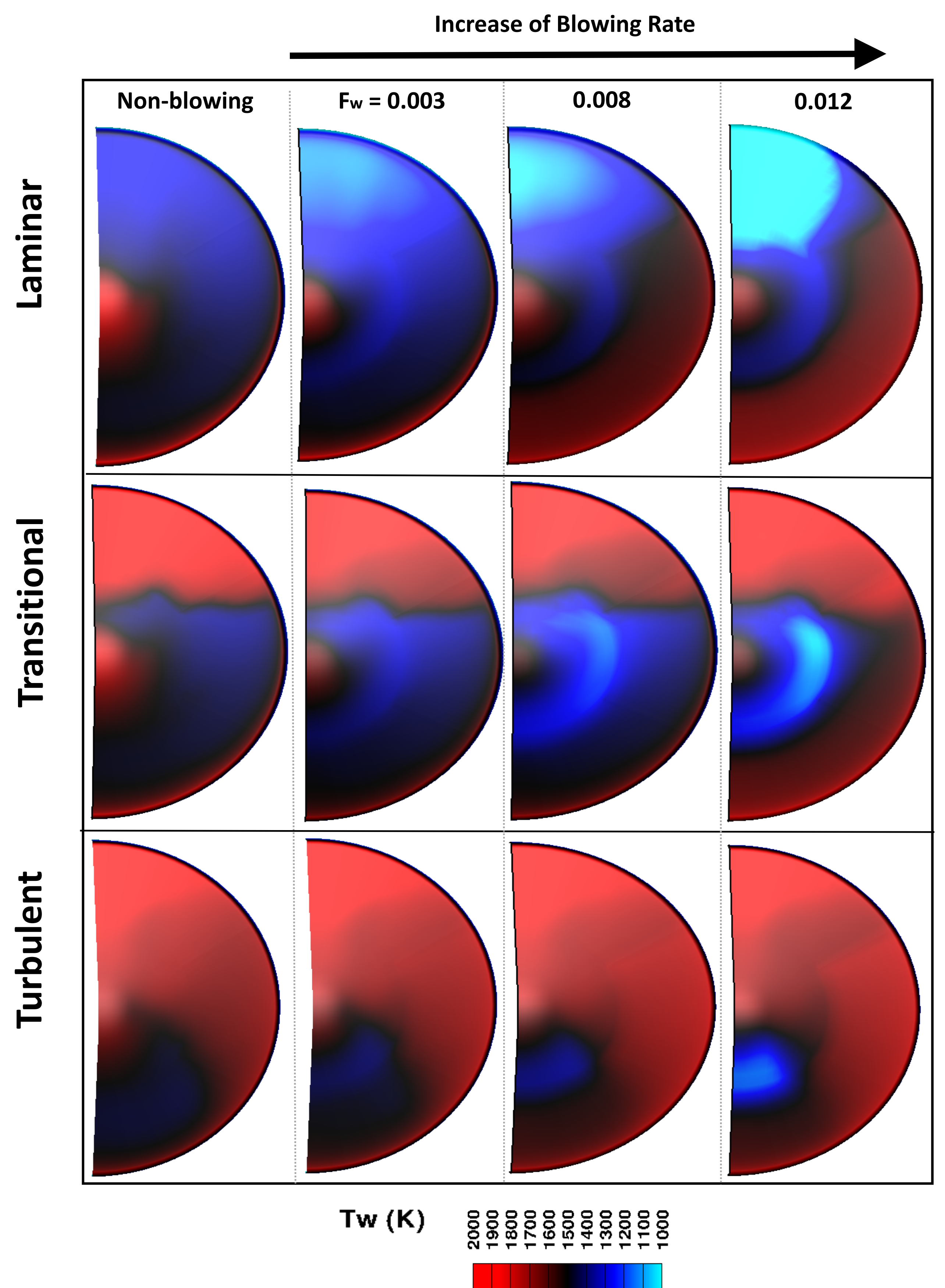


Fig. 5 Wall temperature contour plots of half-body heatshield in laminar, transitional and turbulent regimes with different blowing factor for Scenario A (trajectory 74 s)

Conclusion & Outlook

The effects of injecting pyrolysis gases into the boundary layer, and of transition onset on the aero-heating budget in hypersonic boundary layers are examined by a series of numerical experiments. Out-gassing alters the transition location toward the windside of the forebody of the heatshield. At the same blowing rate, laminar solutions experience more surface cooling than turbulent counterparts. Next step is to implement a model that injects species that have comparable molecular weight to pyrolysis gases such as CO, to represent ablation products .

References

- [1] Schneider, S. P. (2010), J. Spacecr. Rockets 47, 225-237.
- [2] Milos, F.S. & Chen, Y. K. (2013), J. Spacecr. Rockets 50, 137-149.
- [3] Duffa, G. (2013), Ablative Thermal Protection System Modeling.
- [4] Dhawan, S. & Narasimha, R. (1958), J. Fluid Mech. 3, 418-436.
- [5] Wright, M. J. et al. (2009), NASA TM-2009-215388.
- [6] Cruden, B. A. et al. (2013), AIAA Journal 2502.
- [7] Menter F. R. et al. (2015), Flow Turb. Comb, 95, 583-619.
- [8] Edquist K. T. et al. (2013), AIAA Thermophys. 44, p13.